ACS chemical biology

Letters

pubs.acs.org/acschemicalbiology

Argininosuccinate Synthase 1 is a Metabolic Regulator of Colorectal Cancer Pathogenicity

Leslie A. Bateman,[†] Wan-Min Ku, Martin J. Heslin,[‡] Carlo M. Contreras,[‡] Christine F. Skibola,*[,‡] and Daniel K. Nomura*[,†]

[†]Departments of Chemistry, Molecular and Cell Biology, and Nutritional Sciences and Toxicology, University of California, Berkeley, Berkeley, California 94720, United States

[‡]The University of Alabama at Birmingham, Birmingham, Alabama 35233, United States

Supporting Information

ABSTRACT: Like many cancer types, colorectal cancers have dysregulated metabolism that promotes their pathogenic features. In this study, we used the activity-based protein profiling chemoproteomic platform to profile cysteine-reactive metabolic enzymes that are upregulated in primary human colorectal tumors. We identified argininosuccinate synthase 1 (ASS1) as an upregulated target in primary human colorectal tumors and show that pharmacological inhibition or genetic ablation of ASS1 impairs colorectal cancer pathogenicity. Using metabolomic profiling, we show that ASS1 inhibition leads to reductions in the levels of oncogenic metabolite fumarate, leading to impairments in glycolytic metabolism that supports colorectal cancer cell pathogenicity. We show here that ASS1 inhibitors may represent a novel therapeutic approach for attenuating colorectal cancer through compromising critical metabolic and metabolite signaling pathways and demonstrate the utility of coupling chemoproteomic and metabolomic strategies to map novel metabolic regulators of cancer.

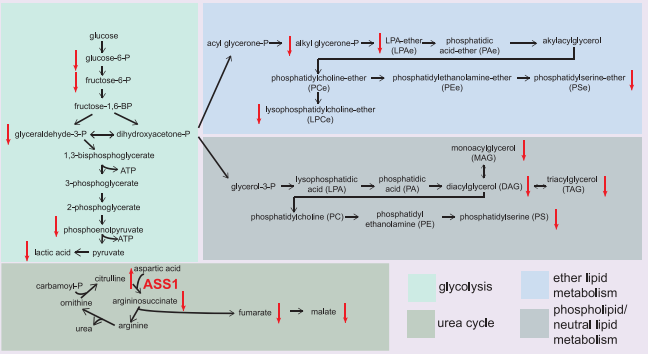

Cancer cells show dysregulated metabolism that underlies nearly every aspect of cancer pathogenicity. Among various cancers, nearly 50 000 people are expected to die from colorectal cancers with ~135 000 new estimated cases in 2016, making colorectal cancer the second most lethal cancer type, and thus new therapeutic targets need to be discovered to reduce this mortality rate associated with colorectal cancers.

Here, we used a chemoproteomic strategy called activity-based protein profiling (ABPP) to map dysregulated metabolic enzyme targets that are important in colorectal cancer. ABPP uses reactivity-based chemical probes to map proteome-wide reactive, ligandable, and functional sites directly in complex proteomes.[1−3] This strategy can be used to identify dysregulated protein targets in cancer, as well as sites of probe labeling which can potentially constitute ligandable sites or a binding pocket where small-molecule ligands may bind.[4,5] These reactive and ligandable sites of probe modification may in turn be pharmacologically interrogated using various strategies such as covalent ligand discovery methods.[4]

Here, we used a broad cysteine-reactive iodoacetamide-alkyne (IAyne) probe to map dysregulated protein targets in primary human colorectal tumors compared to their matched normal colorectal tissue counterparts (Figure 1A; Table S1).[5,6] We labeled colorectal tumor and normal colorectal tissue proteomes with the cysteine-reactive iodoacetamide-alkyne (IAyne) probe followed by conjugation of a biotin handle by copper-catalyzed azide−alkyne cycloaddition (CuAAC), avidin-enrichment, and proteomic profiling (Figure 1A,B; Table S1). We profiled cysteine reactivity in this study due to its functional importance in many types of metabolic enzymes, including the role of cysteine in enzyme catalysis, redox regulation, allosteric modulation, and metal binding.[7] Proteomic analysis of probe-enriched protein targets yielded 555 total proteins. We then filtered these proteins for metabolic enzymes that were significantly heightened (p < 0.01, >2-fold) in primary colorectal tumors compared to matched normal tissue counterparts, resulting in 10 lead metabolic enzyme candidates for further study. These targets included NNMT, IMPDH2, NT5C2, GMPS, FASN, NME1, COMT, GART, GPX2, and ASS1 (Figure 1B).

Due to limited amounts of tumor tissue, we could not perform detailed studies to quantitatively elucidate probe modification sites of cysteines labeled by IAyne on individual tumors and normal tissues. Instead, we performed isotopic tandem orthogonal proteolysis-enabled ABPP (isoTOP-ABPP) studies on pooled colorectal tumor tissue to quantitatively map cysteine reactivity in primary human colorectal tumors. We labeled pooled colorectal tumors with 100 μM versus 10 μM of IAyne,

Received: December 29, 2016
Accepted: February 23, 2017
Published: February 23, 2017

DOI: 10.1021/acschembio.6b01158
ACS Chem. Biol. XXXX, XXX, XXX−XXX

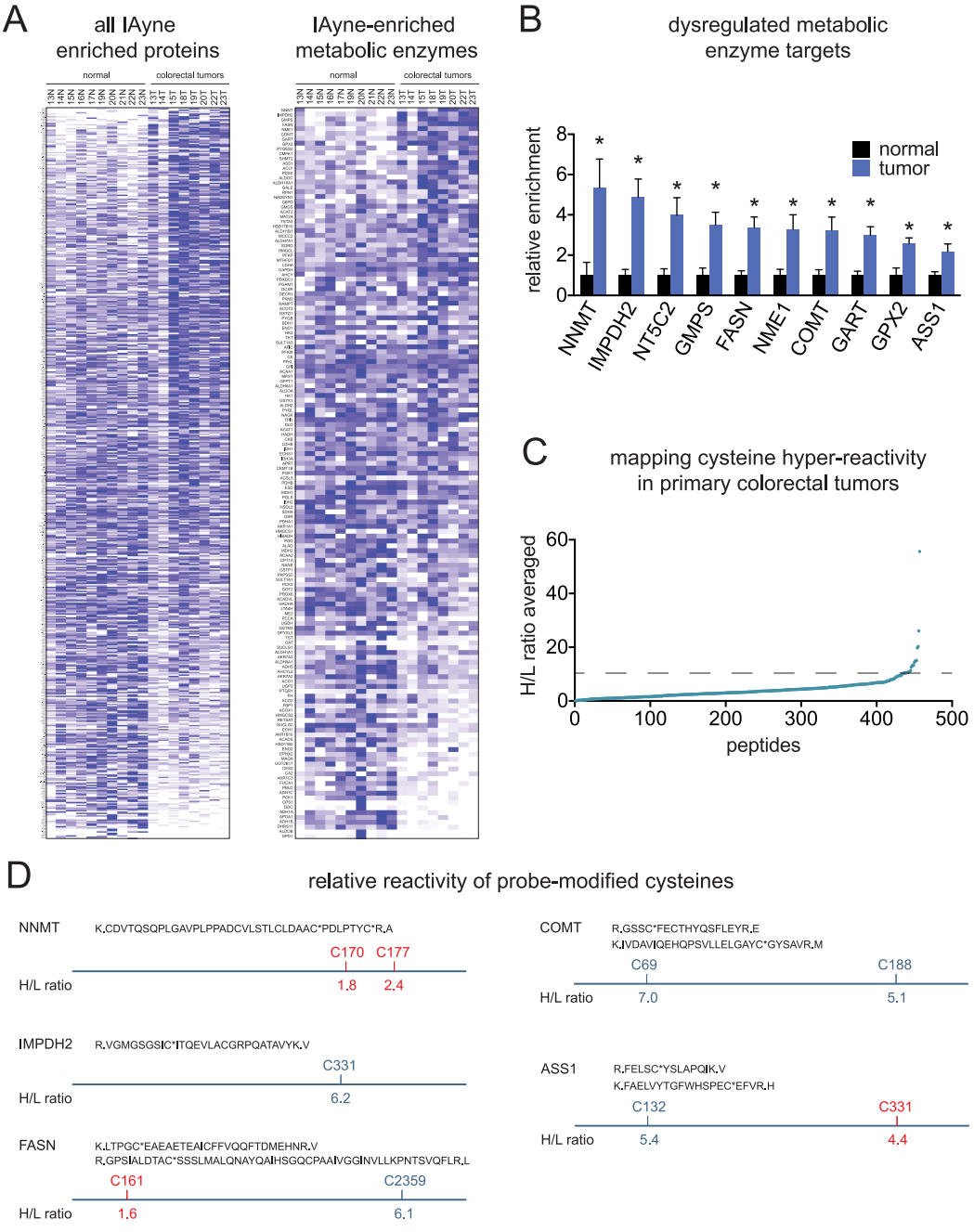

Figure 1. Profiling dysregulated metabolic enzyme targets in colorectal tumors. (A) ABPP analysis mapping cysteine reactivity of primary human colorectal tumor and normal colorectal tissue proteomes. Proteomes were labeled with the cysteine-reactive iodoacetamide-alkyne (IAyne) probe (10 μM) or DMSO (for no-probe control) and subjected to copper-catalyzed azide−alkyne cycloaddition to append on biotin-azide. Probe-labeled proteins were subsequently avidin-enriched and digested, and tryptic peptides were analyzed by proteomic methods. IAyne enriched protein targets were quantified by spectral counting. Heatmap denotes relative levels of each protein in each tumor. Dark blue indicates higher relative protein level compared to white or lighter blue. Shown on the left are all proteins enriched by IAyne (>2-fold over no-probe control). Shown on the right are just the metabolic enzymes enriched by IAyne. (B) Dysregulated metabolic enzyme targets. Metabolic enzyme targets from Figure 1A that were significantly ($p < 0.01$) upregulated by greater than 2-fold in primary human colorectal tumors compared to normal colorectal tissues. (C) IsoTOP-ABPP analysis of cysteine reactivity in pooled primary human colorectal tumors. Pooled primary human colorectal tumors were labeled with 100 μM or 10 μM IAyne and then subjected to copper-catalyzed azide−alkyne cycloaddition to append a biotin-azide handle bearing an isotopically heavy (for 100 μM IAyne labeling) or light (for 10 μM IAyne labeling) and a TEV protease recognition site. Then, 100 μM and 10 μM probe-labeled proteins were mixed in a 1:1 ratio, and avidin-enriched, tryptically digested, and tryptic probe-modified peptides were then enriched and released by TEV protease and analyzed by quantitative proteomics. Shown are heavy to light probe-modified tryptic peptide ratios. (D) Relative reactivity of probe-modified cysteines from data shown in C. Data shown in B are average ± SEM. Significance in B is expressed as *$p < 0.01$. Data in B represent $n = 10$ for normal colorectal tissue and $n = 8$ for colorectal tumors. Raw and analyzed cysteine profiling data and isoTOP-ABPP data can be found in Table S1.

DOI: 10.1021/acschembio.6b01158
ACS Chem. Biol. XXXX, XXX, XXX−XXX

followed by appendage of an isotopically heavy (100 μM) or light (10 μM) biotin-azide analytical handle that bears a TEV protease cleavage site. Upon combining high versus low probe-treated proteomes in a 1:1 ratio, we then enriched probe-modified tryptic peptides and analyzed heavy to light peptide ratios by quantitative proteomic methods (Figure 1C; Table S1). In total, we identified 443 probe-modified tryptic peptides from primary human colorectal tumors. Those peptides that show stoichiometric IAyne labeling resulting in heavy to light ratios of ~10 are not considered hyper-reactive. In contrast, those probe-modified peptides that show heavy to light isotopic ratios of <3−5 indicate sites that were preferentially labeled to completion at the lower (10 μM) compared to higher (100 μM) probe concentration, suggesting that these cysteines are hyper-reactive (Figure 1C; Table S1). Previous studies have used this isoTOP-ABPP approach to quantitatively map cysteine reactivity and have shown that these hyper-reactive sites are enriched in functional cysteines.[5] We mapped the relative reactivity of the probe-modified cysteines for the dysregulated metabolic enzyme targets that we could identify in the isoTOP-ABPP experiment. While we were not able to identify the probe-modification sites for all 10 lead metabolic enzyme targets, we show several potential hyper-reactive cysteines on these targets, including the active-site cysteine C161 on FASN as well as unannotated cysteines C170 and C177 on NNMT and C331 on ASS1 (Figure 1D; Table S1). These unannotated cysteines may represent potential ligandable sites for future pharmacological interrogation of these enzymes.

Most of these enzymes have been previously demonstrated to be important in cancer, including NNMT, IMPDH2, NT5C2, GMPS, FASN, NME1, COMT, GART, and GPX2.[8−16] ASS1 has been shown to be silenced in various types of tumors, including myxofibrosarcomas; melanoma; liver, renal, pancreatic, bladder, and nasopharyngeal cancers; osteosarcomas; and prostate cancers to act as a tumor suppressor.[17−22] The role of ASS1-deficiency in these tumors has been previously shown to cause diversion of aspartate to pyrimidine synthesis.[17,18] However, ASS1 has also been shown to be increased in expression in certain tumor types, including colorectal, ovarian, stomach, and lung cancers, but the role of ASS1 increased expression in cancer is not well understood.[18,23−25] Thus, we decided to focus on investigating the role of ASS1 in colorectal cancer cells.

Treatment of SW620 colorectal cancer cells with the ASS1 inhibitor *N*-methyl-DL-aspartic acid (MDLA) leads to impaired proliferation and serum-free survival (Figure 2A). We also knocked down the expression of ASS1 using two independent short-hairpin oligonucleotides and show that ASS1 knockdown also causes impairments in proliferation and survival as well as *in vivo* tumor xenograft growth in mice (Figure 2B,C). These studies show that ASS1 inhibition impairs colorectal cancer pathogenicity.

To better understand the mechanisms underlying the role of ASS1 in colorectal cancer, we performed metabolomic profiling of SW620 cells treated with MDLA (Figure 3A−C; Table S2). We used a single-reaction-monitoring (SRM)-based liquid chromatography−mass spectrometry (LC-MS/MS) platform to measure the relative levels of 231 metabolites spanning glycolysis, the pentose phosphate pathway (PPP), the tricarboxylic acid (TCA) cycle, nucleotides, inositols, the urea cycle, polyamines, amino acids, hexosamines, cofactors, fatty acids, neutral lipids, acylethanolamines, acyl carnitines, acyltaurines, sphingolipids, phospholipids, ether lipids, and sterols and

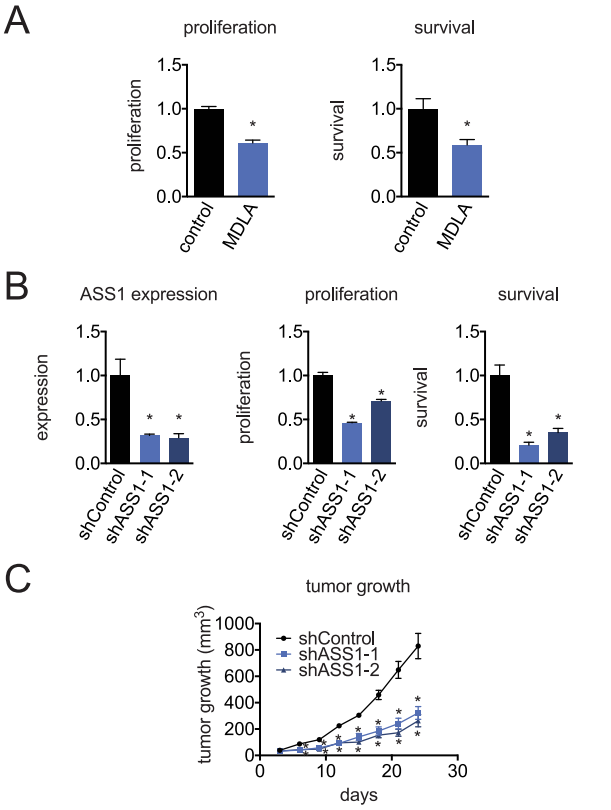

Figure 2. Role of ASS1 in colorectal cancer pathogenicity. (A) SW620 proliferation and serum-free cell survival. SW620 cells were treated with water or MDLA for 48 h, and proliferation and survival were assessed by Hoescht staining. (B) ASS1 expression and proliferation and survival in SW620 cells. ASS1 expression was knocked down with two independent shRNA oligonucleotides. Expression was assessed by qPCR. Proliferation and survival were assessed 48 h after seeding by Hoescht staining. (C) Tumor xenograft growth of SW620 cells in immune-deficient SCID mice. SW620 shControl and shASS1 cells were subcutaneously injected into SCID mice, and tumor growth was measured. Data shown as average ± SEM. Significance is expressed as $^*p < 0.05$. Data represent n = 4−6/group.

steroids. Through this profiling effort, we identified a unique metabolomic signature arising from ASS1 inhibition by MDLA in SW620. Expectedly, we observed the ASS1 substrate citrulline and ASS1 product argininosuccinate increased and decreased in levels, respectively, upon MDLA treatment (Figure 3B,C). Intriguingly, we also observed decreased levels of fumarate and malate. Fumarate can arise in the mitochondria from the TCA cycle or in the cytosol from the urea cycle downstream of ASS1 and can be converted to malate in the cytosol. Since no other TCA cycle metabolite was decreased upon MDLA treatment, we postulated that this fumarate reduction was likely due to inhibition of the urea cycle, rather than impairment in the TCA cycle. Interestingly, fumarate has been shown to be a tumor-suppressing signaling metabolite that can inhibit hypoxia-inducible factor (HIF) prolyl 4-hydroxylases leading to degradation of HIF and impairment of glycolytic metabolism.[26,27] We thus postulated that reductions in fumarate caused by ASS1 inhibition may impair glycolytic metabolism. Consistent with this premise, we observed reductions in the levels of several glycolytic intermediates (Figure 3B,C). Acylglycerolipid and ether lipid metabolism also branch off from glycolysis from dihydroxyacetone phosphate-mediated generation of glycerol-3-phosphate and

DOI: 10.1021/acschembio.6b01158
ACS Chem. Biol. XXXX, XXX, XXX−XXX

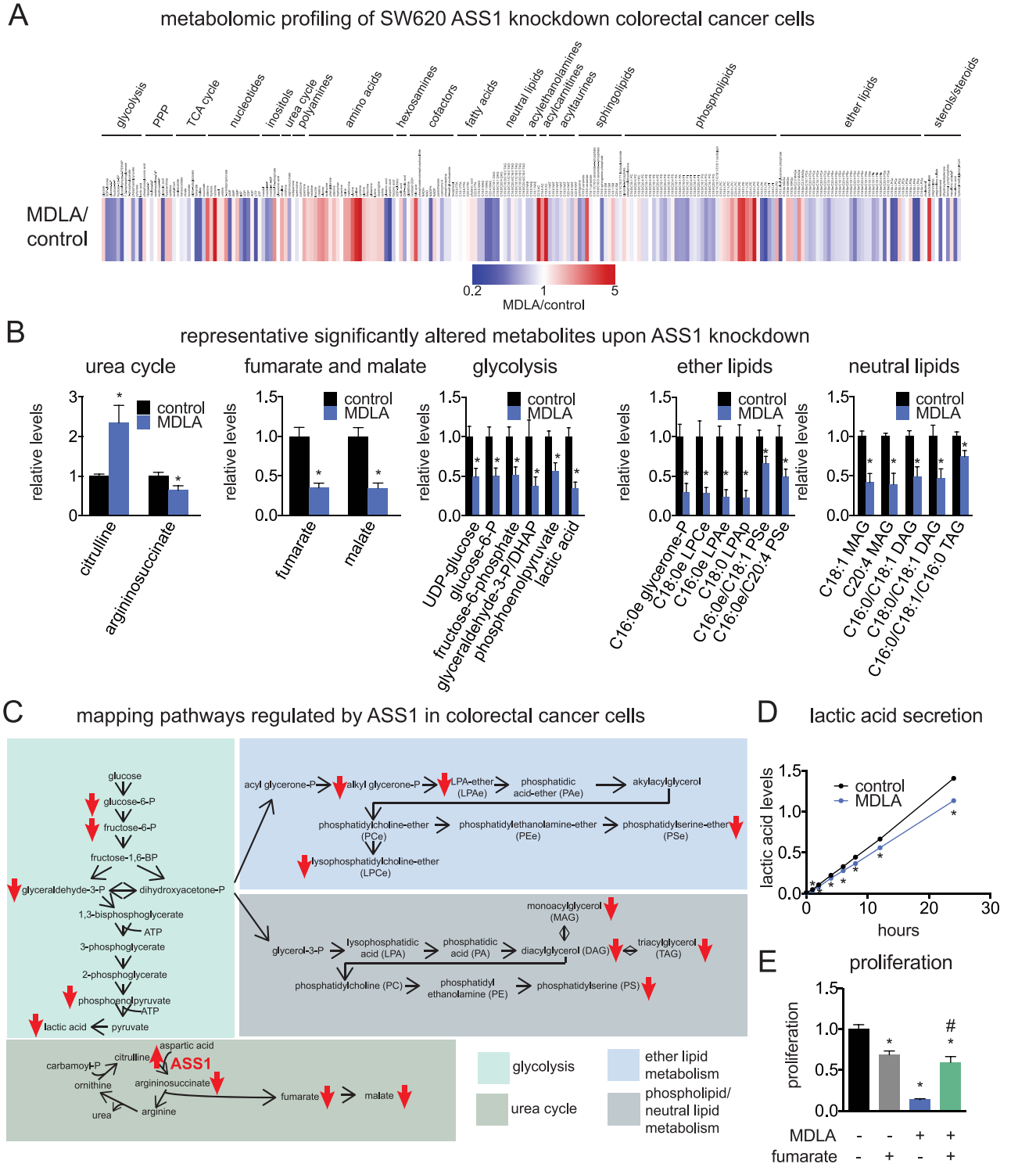

Figure 3. Functional metabolomic profiling and pathway mapping of ASS1 inhibition in colorectal cancer cells. (A) Metabolomic profiling of MDLA-treated SW620 cells. SW620 cells were treated with water or MDLA (5 mM) for 4 h, and relative metabolite levels were measured using SRM-based LC-MS/MS. Heatmap shows relative changes or MDLA to control ratios for each metabolite, where red indicates that MDLA increased the level of the metabolite, white indicates no change, and blue indicates that MDLA reduced the level of the metabolite. (B) Levels of representative significantly changing metabolites shown grouped by pathways. (C) Mapping metabolic changes to a pathway map. (D) Lactic acid secretion. SW620 cells were treated with water or MDLA (5 mM), and lactic acid levels were measured at the designated time points. (E) SW620 cell proliferation. SW620 cells were treated with water, MDLA (5 mM), or MDLA (5 mM) and fumarate (1 mM), and proliferation was measured after 48 h by Hoescht staining. Data shown as average ± SEM. Significance is expressed as $*p < 0.05$. Data represent $n = 8$/group. More details on the metabolomics data can be found in Table S2.

alkylglyceronephosphate, respectively. Likely stemming from the impairments in glycolytic metabolism, we also observed reductions in the levels of acylglycerophospholipids, neutral lipids, and ether lipids, including key oncogenic signaling lipids

DOI: 10.1021/acschembio.6b01158
ACS Chem. Biol. XXXX, XXX, XXX−XXX

that act on lysophosphatidic acid receptors—lysophosphatidic acid-ether (LPAe) and LPA-plasmalogen (LPAp; Figure 3B,C). We have previously shown that inhibition of alkylglycerone phosphate synthase, the rate limiting enzyme in ether lipid synthesis, lowered the levels of several key ether lipids, including LPAe and LPAp levels, leading to impaired cancer pathogenicity.[28] We further show that MDLA treatment in SW620 cells significantly impairs lactic acid secretion (Figure 3D), providing further evidence that ASS1 inhibition impairs glycolysis. Consistent with the role of reduction of fumarate in the proliferative impairments observed with ASS1 inhibition, we also show substantial rescue in the antiproliferative effects observed with MDLA treatment when cotreated with fumarate in SW620 cells (Figure 3E).

In conclusion, our data point to ASS1 as a colorectal cancer target that, when inhibited, lowers the levels of the tumor-suppressing metabolite fumarate leading to impaired cancer cell glycolytic and lipid metabolism that underlies colorectal cancer pathogenicity. While the interpretations that we present here are based on the metabolomic changes that we observe with ASS1 inhibition in colorectal cancer cells, we expect that there are alternate mechanisms involved that may have been missed in our metabolomics profiling efforts. Now that we have identified potential reactive nucleophilic and ligandable sites within ASS1 using isoTOP-ABPP strategies, it would be interesting to perform small-molecule screening efforts against this site, toward developing more potent ASS1 inhibitors. While we could not perform additional metabolomic studies with our ASS1 knockdown lines due to the viability impairments that arose from long-term culturing of ASS1 knockdown cells, it would be of future interest to recapitulate the metabolic results from our studies with inducible knockdown or knockout cell or animal models of ASS1. Our results also demonstrate the utility of combining chemoproteomic and metabolomic strategies toward identifying important metabolic pathways that support cancer pathogenicity.

EXPERIMENTAL PROCEDURES

Chemicals. IAyne was obtained from CHESS Gmbh. Heavy and light TEV-biotin tags were synthesized according to previously described methods.[5,29] MDLA was purchased from Sigma.

Cell Culture. SW620 cells were purchased from ATCC. SW620 cells were grown in L-15 media with 10% fetal bovine serum (FBS) in ambient CO_2.

ASS1 Knockdown. Targets were knocked down transiently with siRNA or stably with shRNA as previously described.[30] For siRNA studies, SW620 cells (200 000 cells/well) were seeded overnight, after which siControl (nontargeting siRNA) or siASS1 siRNA oligonucleotides (five pooled siRNAs targeting each target purchased from Dharmacon) were transfected into cells using Dharmafect 1. Cells were harvested after 48 h for qPCR and for seeding for cell viability assays.

For shRNA studies, shControl (targeting GFP) and shASS1 constructs (purchased from Sigma) were transfected into HEK293T cells alongside lentiviral vectors using FuGENE. Lentivirus was collected and used to infect the target cancer cell line with Polybrene (0.01 mg mL^{-1}). Infected cells were then selected for with 1 mg mL^{-1} puromycin. The short-hairpin sequences used for generation of the ASS1 knockdown lines were

shASS1−1—CCGGATGAACGTGCAGGGTGATTATCTCGAGATAATCACCCTGCACGTTCATTTTTTTG

shASS1−2—CCGGCCCAAGTACAGGCGCTAATTGCTCGAGCAATTAGCGCCTGTACTTGGGTTTTTTG.

The control shRNA target sequence was GCAAGCTGACCCTGAAGTTCAT. qPCR was used to confirm knockdown using previously reported methods.[31]

Cellular Phenotype Studies. Cell proliferation and serum-free cell survival were performed as previously described.[31] Cell survival measures cell death under serum-free and nonproliferative conditions, whereas cell proliferation assays are performed in the presence of serum and measures proliferation of cells.

Tumor Xenograft Studies. Human tumor xenografts were established by injecting 100 μL of cancer cells at a concentration of 2.0×10^4 cells/μL ectopically into the flank of C.B17 severe combined immunodeficiency (SCID) mice (Taconic Farms), and tumors were measured using calipers as previously described.[31]

Metabolomic Profiling of Cancer Cells. Metabolomic analyses were conducted using previously described methods.[32] For nonpolar metabolomic analyses, flash frozen cell pellets were extracted in 4 mL of 2:1:1 chloroform/methanol/PBS with internal standards dodecylglycerol (10 nmol) and pentadecanoic acid (10 nmol). Organic and aqueous layers were separated by centrifugation, and the organic layer was extracted. The aqueous layer was acidified with 0.1% formic acid followed by re-extraction with 2 mL of chloroform. The second organic layer was combined with the first extract and dried under nitrogen, after which lipids were resuspended in chloroform (120 μL). A 10 μL aliquot was then analyzed by single-reaction monitoring (SRM)-based LC-MS/MS. For polar metabolomics, cell pellets were extracted in 40:40:20 acetonitrile/methanol/water with internal standard d_3 N^{15}-serine (1 nmol). The extracts were vortexed and sonicated, and after centrifugation, an aliquot of the polar metabolite fraction (supernatant) was then analyzed by single-reaction monitoring (SRM)-based LC-MS/MS. Relative levels of metabolites were quantified by integrating the area under the curve for each metabolite, normalizing to internal standard values and then normalizing to the average values of the control groups.

Lactic Acid Secretion and Glucose Consumption. Lactic acid secretion and glucose consumption were assessed using kits purchased from Abcam per the manufacturers' protocols.

Cysteine Reactivity Profiling. Cysteine reactivity profiling was performed as previously described.[32,33] A total of 1 mg of normal or tumor tissue proteome was incubated with iodoacetamide-alkyne (10 μM) for 30 min at RT. Following incubation, biotin-azide was appended by CuAAC, and probe-labeled proteins were enriched, digested with trypsin, and analyzed by LC-LC/MS/MS as previously described.[32,33] Total peptides from each proteomic experiment were pressure-loaded onto 250 μm inner diameter fused silica capillary tubing packed with 4 cm of Aqua C18 reverse-phase resin (Phenomenex # 04A-4299). The samples were then attached using a MicroTee PEEK 360 μm fitting (Thermo Fisher Scientific #p-888) to a 13 cm laser pulled column packed with 10 cm Aqua C18 reverse-phase resin and 3 cm of strong-cation exchange resin for isoTOP-ABPP studies. Samples were analyzed using a Thermo LTQ-XL using a Multidimensional Protein Identification Technology (MudPIT) program as previously described.[5] These methods are identical to our previously validated methods.[32,33] Biological variability in total spectral counts were less than 30%. The instrument was calibrated daily, and calibrant sensitivity was within 10% during these runs. The raw proteomic data for these experiments can be found in Table S1.

IsoTOP-ABPP Analysis. IsoTOP-ABPP analyses were performed as previously described.[5] Primary human tumor samples were labeled with IAyne (100 or 10 μM) for 1 h at RT. They were subsequently treated with isotopically light (10 μM) or heavy (100 μM) TEV-biotin, and CuAAC was performed as previously described.[5] For analysis of cysteine reactivity in primary colorectal tumor tissue, tumors were pooled and incubated with either 100 μM IAyne and isotopically heavy TEV-biotin or 10 μM IAyne and isotopically light TEV-biotin followed by CuAAC as previously described.[5] Probe-labeled proteins were subsequently avidin-enriched and digested with trypsin, and probe-modified tryptic peptides were subsequently isolated and released by TEV protease as previously described.[5,34] Resulting peptides were collected and stored at −80 °C until analysis.

DOI: 10.1021/acschembio.6b01158
ACS Chem. Biol. XXXX, XXX, XXX−XXX

Peptides from all proteomic experiments were pressure-loaded onto 250 μm inner diameter fused silica capillary tubing packed with 4 cm of Aqua C18 reverse-phase resin (Phenomenex # 04A-4299). The samples were then attached using a MicroTee PEEK 360 μm fitting (Thermo Fisher Scientific #p-888) to a 13 cm laser pulled column packed with 10 cm Aqua C18 reverse-phase resin and 3 cm of strong-cation exchange resin for isoTOP-ABPP studies. Samples were analyzed using a Q Exactive Plus mass spectrometer (Thermo Fisher Scientific) using a Multidimensional Protein Identification Technology (MudPIT) program as previously described.[5] Data were collected in data-dependent acquisition mode with dynamic exclusion enabled (60 s). One full MS (MS1) scan (400−1800 m/z) was followed by 15 MS2 scans (ITMS) of the nth most abundant ions. Heated capillary temperature was set to 200 °C, and the nanospray voltage was set to 2.75 kV.

For MudPIT runs, samples were run with the following five-step MudPIT program (using 0%, 10%, 25%, 80%, and 100% salt bumps). Data were extracted in the form of MS1 and MS2 files using Raw Extractor 1.9.9.2 (Scripps Research Institute) and searched against the Uniprot mouse database using ProLuCID search methodology in IP2 v.3 (Integrated Proteomics Applications, Inc.).[35] Cysteine residues were searched with a static modification for carboxyaminomethylation (+57.02146) and up to two differential modifications for either the light or heavy TEV tags (+464.28596 or +470.29977, respectively). Peptides were required to have at least one tryptic end and to contain the TEV modification. These methods are identical to well-validated methods described previously.[4,5,34] ProLUCID data were filtered through DTASelect to achieve a peptide false-positive rate below 1%. MS/MS data for the probe-modified peptides shown in Figure 1D were manually interpreted and confirmed. The raw proteomic data for isoTOP-ABPP experiments can be found in Table S1.

Primary Human Colorectal Tumors. Eligible patients completed written consent for our tissue banking protocol that is approved by the University of Alabama at Birmingham Institutional Review Board. During the pancreatic resection, a 1 cm^3 portion of the tumor was dissected free of the fresh resection specimen, divided into 4−5 aliquots, placed into 1.5 mL cryovials, flash frozen, and stored at −80 °C. Adjacent nontumor bearing pancreas tissue was also collected and banked in a similar manner.

■ ASSOCIATED CONTENT

Ⓢ Supporting Information

The Supporting Information is available free of charge on the ACS Publications website at DOI: 10.1021/acschembio.6b01158.

Table legends for Tables S1 and S2(PDF)
Table S1 (XLSX)
Table S2 (XLSX)

■ AUTHOR INFORMATION

Corresponding Authors

*E-mail: cskibola@uab.edu.
*E-mail: dnomura@berkeley.edu.

ORCID

Daniel K. Nomura: 0000-0003-1614-8360

Notes

The authors declare no competing financial interest.

■ ACKNOWLEDGMENTS

We thank the members of the Nomura Research Group for critical reading of the manuscript. This work was supported by grants from the National Institutes of Health (R01CA172667 for D.K.N. and L.A.B.), American Cancer Society Research Scholar Award (RSG14-242-01-TBE for D.K.N. and L.A.B.), DOD Breakthroughs Award (CDMRP W81XWH-15-1-0050 for D.K.N. and L.A.B.).

■ REFERENCES

(1) Medina-Cleghorn, D., and Nomura, D. K. (2014) Exploring metabolic pathways and regulation through functional chemoproteomic and metabolomic platforms. *Chem. Biol. 21*, 1171−1184.
(2) Nomura, D. K., Dix, M. M., and Cravatt, B. F. (2010) Activity-based protein profiling for biochemical pathway discovery in cancer. *Nat. Rev. Cancer 10*, 630−638.
(3) Roberts, A. M., Ward, C. C., and Nomura, D. K. (2016) Activity-based protein profiling for mapping and pharmacologically interrogating proteome-wide ligandable hotspots. *Curr. Opin. Biotechnol. 43*, 25−33.
(4) Backus, K. M., Correia, B. E., Lum, K. M., Forli, S., Horning, B. D., González-Páez, G. E., Chatterjee, S., Lanning, B. R., Teijaro, J. R., Olson, A. J., Wolan, D. W., and Cravatt, B. F. (2016) Proteome-wide covalent ligand discovery in native biological systems. *Nature 534*, 570−574.
(5) Weerapana, E., Wang, C., Simon, G. M., Richter, F., Khare, S., Dillon, M. B. D., Bachovchin, D. A., Mowen, K., Baker, D., and Cravatt, B. F. (2010) Quantitative reactivity profiling predicts functional cysteines in proteomes. *Nature 468*, 790−795.
(6) Shannon, D. A., and Weerapana, E. (2015) Covalent protein modification: the current landscape of residue-specific electrophiles. *Curr. Opin. Chem. Biol. 24*, 18−26.
(7) Pace, N. J., and Weerapana, E. (2013) Diverse functional roles of reactive cysteines. *ACS Chem. Biol. 8*, 283−296.
(8) Ulanovskaya, O. A., Zuhl, A. M., and Cravatt, B. F. (2013) NNMT promotes epigenetic remodeling in cancer by creating a metabolic methylation sink. *Nat. Chem. Biol. 9*, 300−306.
(9) Zhou, L., Xia, D., Zhu, J., Chen, Y., Chen, G., Mo, R., Zeng, Y., Dai, Q., He, H., Liang, Y., Jiang, F., and Zhong, W. (2014) Enhanced expression of IMPDH2 promotes metastasis and advanced tumor progression in patients with prostate cancer. *Clin. Transl. Oncol. 16*, 906−913.
(10) Tzoneva, G., Perez-Garcia, A., Carpenter, Z., Khiabanian, H., Tosello, V., Allegretta, M., Paietta, E., Racevskis, J., Rowe, J. M., Tallman, M. S., Paganin, M., Basso, G., Hof, J., Kirschner-Schwabe, R., Palomero, T., Rabadan, R., and Ferrando, A. (2013) Activating mutations in the NT5C2 nucleotidase gene drive chemotherapy resistance in relapsed ALL. *Nat. Med. 19*, 368−371.
(11) Reddy, B. A., van der Knaap, J. A., Bot, A. G. M., Mohd-Sarip, A., Dekkers, D. H. W., Timmermans, M. A., Martens, J. W. M., Demmers, J. A. A., and Verrijzer, C. P. (2014) Nucleotide biosynthetic enzyme GMP synthase is a TRIM21-controlled relay of p53 stabilization. *Mol. Cell 53*, 458−470.
(12) Menendez, J. A., and Lupu, R. (2007) Fatty acid synthase and the lipogenic phenotype in cancer pathogenesis. *Nat. Rev. Cancer 7*, 763−777.
(13) Saha, A., and Robertson, E. S. (2011) Functional modulation of the metastatic suppressor Nm23-H1 by oncogenic viruses. *FEBS Lett. 585*, 3174−3184.
(14) Wu, W., Wu, Q., Hong, X., Zhou, L., Zhang, J., You, L., Wang, W., Wu, H., Dai, H., and Zhao, Y. (2015) Catechol-O-methyltransferase, a new target for pancreatic cancer therapy. *Cancer Sci. 106*, 576−583.
(15) Bronder, J. L., and Moran, R. G. (2002) Antifolates targeting purine synthesis allow entry of tumor cells into S phase regardless of p53 function. *Cancer Res. 62*, 5236−5241.
(16) Naiki, T., Naiki-Ito, A., Asamoto, M., Kawai, N., Tozawa, K., Etani, T., Sato, S., Suzuki, S., Shirai, T., Kohri, K., and Takahashi, S. (2014) GPX2 overexpression is involved in cell proliferation and prognosis of castration-resistant prostate cancer. *Carcinogenesis 35*, 1962−1967.
(17) Rabinovich, S., Adler, L., Yizhak, K., Sarver, A., Silberman, A., Agron, S., Stettner, N., Sun, Q., Brandis, A., Helbling, D., Korman, S., Itzkovitz, S., Dimmock, D., Ulitsky, I., Nagamani, S. C. S., Ruppin, E., and Erez, A. (2015) Diversion of aspartate in ASS1-deficient tumours fosters de novo pyrimidine synthesis. *Nature 527*, 379−383.
(18) Delage, B., Fennell, D. A., Nicholson, L., McNeish, I., Lemoine, N. R., Crook, T., and Szlosarek, P. W. (2010) Arginine deprivation and

DOI: 10.1021/acschembio.6b01158
ACS Chem. Biol. XXXX, XXX, XXX−XXX

argininosuccinate synthetase expression in the treatment of cancer. *Int. J. Cancer 126*, 2762−2772.
(19) Huang, H.-Y., Wu, W.-R., Wang, Y.-H., Wang, J.-W., Fang, F.-M., Tsai, J.-W., Li, S.-H., Hung, H.-C., Yu, S.-C., Lan, J., Shiue, Y.-L., Hsing, C.-H., Chen, L.-T., and Li, C.-F. (2013) ASS1 as a novel tumor suppressor gene in myxofibrosarcomas: aberrant loss via epigenetic DNA methylation confers aggressive phenotypes, negative prognostic impact, and therapeutic relevance. *Clin. Cancer Res. 19*, 2861−2872.
(20) Lan, J., Tai, H.-C., Lee, S.-W., Chen, T.-J., Huang, H.-Y., and Li, C.-F. (2014) Deficiency in expression and epigenetic DNA Methylation of ASS1 gene in nasopharyngeal carcinoma: negative prognostic impact and therapeutic relevance. *Tumor Biol. 35*, 161−169.
(21) Kobayashi, E., Masuda, M., Nakayama, R., Ichikawa, H., Satow, R., Shitashige, M., Honda, K., Yamaguchi, U., Shoji, A., Tochigi, N., Morioka, H., Toyama, Y., Hirohashi, S., Kawai, A., and Yamada, T. (2010) Reduced argininosuccinate synthetase is a predictive biomarker for the development of pulmonary metastasis in patients with osteosarcoma. *Mol. Cancer Ther. 9*, 535−544.
(22) Allen, M. D., Luong, P., Hudson, C., Leyton, J., Delage, B., Ghazaly, E., Cutts, R., Yuan, M., Syed, N., Lo Nigro, C., Lattanzio, L., Chmielewska-Kassassir, M., Tomlinson, I., Roylance, R., Whitaker, H. C., Warren, A. Y., Neal, D., Frezza, C., Beltran, L., Jones, L. J., Chelala, C., Wu, B.-W., Bomalaski, J. S., Jackson, R. C., Lu, Y.-J., Crook, T., Lemoine, N. R., Mather, S., Foster, J., Sosabowski, J., Avril, N., Li, C.-F., and Szlosarek, P. W. (2014) Prognostic and therapeutic impact of argininosuccinate synthetase 1 control in bladder cancer as monitored longitudinally by PET imaging. *Cancer Res. 74*, 896−907.
(23) Shan, Y.-S., Hsu, H.-P., Lai, M.-D., Yen, M.-C., Luo, Y.-P., and Chen, Y.-L. (2015) Increased expression of argininosuccinate synthetase protein predicts poor prognosis in human gastric cancer. *Oncol. Rep. 33*, 49−57.
(24) Shan, Y.-S., Hsu, H.-P., Lai, M.-D., Yen, M.-C., Chen, W.-C., Fang, J.-H., Weng, T.-Y., and Chen, Y.-L. (2015) Argininosuccinate synthetase 1 suppression and arginine restriction inhibit cell migration in gastric cancer cell lines. *Sci. Rep. 5*, 9783.
(25) Rho, J., Qin, S., Wang, J. Y., and Roehrl, M. H. A. (2008) Proteomic expression analysis of surgical human colorectal cancer tissues: up-regulation of PSB7, PRDX1, and SRP9 and hypoxic adaptation in cancer. *J. Proteome Res. 7*, 2959−2972.
(26) Linehan, W. M., and Rouault, T. A. (2013) Molecular pathways: Fumarate hydratase-deficient kidney cancer−targeting the Warburg effect in cancer. *Clin. Cancer Res. 19*, 3345−3352.
(27) Kaelin, W. G. (2011) Cancer and altered metabolism: potential importance of hypoxia-inducible factor and 2-oxoglutarate-dependent dioxygenases. *Cold Spring Harbor Symp. Quant. Biol. 76*, 335−345.
(28) Benjamin, D. I., Cozzo, A., Ji, X., Roberts, L. S., Louie, S. M., Mulvihill, M. M., Luo, K., and Nomura, D. K. (2013) Ether lipid generating enzyme AGPS alters the balance of structural and signaling lipids to fuel cancer pathogenicity. *Proc. Natl. Acad. Sci. U. S. A. 110*, 14912−14917.
(29) Weerapana, E., Speers, A. E., and Cravatt, B. F. (2007) Tandem orthogonal proteolysis-activity-based protein profiling (TOP-ABPP)—a general method for mapping sites of probe modification in proteomes. *Nat. Protoc. 2*, 1414−1425.
(30) Benjamin, D. I., Louie, S. M., Mulvihill, M. M., Kohnz, R. A., Li, D. S., Chan, L. G., Sorrentino, A., Bandyopadhyay, S., Cozzo, A., Ohiri, A., Goga, A., Ng, S.-W., and Nomura, D. K. (2014) Inositol phosphate recycling regulates glycolytic and lipid metabolism that drives cancer aggressiveness. *ACS Chem. Biol. 9*, 1340−1350.
(31) Louie, S. M., Grossman, E. A., Crawford, L. A., Ding, L., Camarda, R., Huffman, T. R., Miyamoto, D. K., Goga, A., Weerapana, E., and Nomura, D. K. (2016) GSTP1 is a Driver of Triple-Negative Breast Cancer Cell Metabolism and Pathogenicity. *Cell Chem. Biol. 23*, 567.
(32) Louie, S. M., Grossman, E. A., Crawford, L. A., Ding, L., Camarda, R., Huffman, T. R., Miyamoto, D. K., Goga, A., Weerapana, E., and Nomura, D. K. (2016) GSTP1 Is a Driver of Triple-Negative Breast Cancer Cell Metabolism and Pathogenicity. *Cell Chem. Biol. 23*, 567−578.
(33) Medina-Cleghorn, D., Bateman, L. A., Ford, B., Heslin, A., Fisher, K. J., Dalvie, E. D., and Nomura, D. K. (2015) Mapping Proteome-Wide Targets of Environmental Chemicals Using Reactivity-Based Chemoproteomic Platforms. *Chem. Biol. 22*, 1394−1405.
(34) Counihan, J. L., Duckering, M., Dalvie, E., Ku, W.-M., Bateman, L. A., Fisher, K. J., and Nomura, D. K. (2017) Chemoproteomic Profiling of Acetanilide Herbicides Reveals Their Role in Inhibiting Fatty Acid Oxidation. *ACS Chem. Biol.*, DOI: 10.1021/acschembio.6b01001.
(35) Xu, T., Park, S. K., Venable, J. D., Wohlschlegel, J. A., Diedrich, J. K., Cociorva, D., Lu, B., Liao, L., Hewel, J., Han, X., Wong, C. C. L., Fonslow, B., Delahunty, C., Gao, Y., Shah, H., and Yates, J. R. (2015) ProLuCID: An improved SEQUEST-like algorithm with enhanced sensitivity and specificity. *J. Proteomics 129*, 16−24.

DOI: 10.1021/acschembio.6b01158
ACS Chem. Biol. XXXX, XXX, XXX−XXX